Modular Smart Molecules for PSMA-Targeted Chemotherapy

Feyisola P. Olatunji[1], **Michael Pun**[1,3,5], **Jacob W. Herman**[1], **Oscar Romero**[1], **Mitchell Maniatopoulos**[1], **Joseph D. Latoche**[2], **Robert A. Parise**[2], **Jianxia Guo**[2], **Jan H. Beumer**[2,6,7], **Carolyn J. Anderson**[3,4,5], **Clifford E. Berkman**[1]

[1]Washington State University, Department of Chemistry, Pullman, WA 99164-4630

[2]Cancer Therapeutics Program, UPMC Hillman Cancer Center, Pittsburgh, PA 15213

[3]Department of Chemistry, University of Missouri, Columbia, MO 65211

[4]Department of Radiology, University of Missouri, Columbia, MO 65211

[5]Molecular Imaging and Theranostics Center, University of Missouri, Columbia, MO 65211

[6]Department of Pharmaceutical Sciences, School of Pharmacy, University of Pittsburgh, PA, 15261.

[7]Division of Hematology-Oncology, Department of Medicine, University of Pittsburgh School of Medicine, Pittsburgh, PA 15261.

Abstract

New targeted chemotherapeutics are urgently needed to minimize off-target toxicity and reduce the high mortality rate associated with metastatic prostate cancer (PCa). Herein, we report on the modular synthesis, pharmacokinetics, and efficacy of two small-molecule drug-conjugates (SMDCs) targeted to prostate-specific membrane antigen (PSMA) incorporating either: (1) a cathepsin-B cleavable valine-citrulline, or (2) an acid-cleavable phosphoramidate linker. Crucial components utilized in the design of the conjugates include: (1) CTT1298, a nanomolar affinity ligand that binds irreversibly to PSMA and has proven in past studies to rapidly internalize and shuttle payloads into PSMA-expressing PCa cells, (2) MMAE, a known potent cytotoxic payload, and (3) an albumin-binder, proven to improve residence time of drug conjugates. At dose of 0.8 mg/kg (~250 nmol/kg), the two SMDCs showed significant efficacy in a PSMA(+) PC3-PIP mouse model of human PCa compared to controls, without inducing systemic toxicity. Though localization of the SMDCs was observed in tissues apart from the tumor, release of

Corresponding authors: Carolyn J. Anderson, University of Missouri, Department of Chemistry, Columbia, MO 65211, carolyn.j.anderson@missouri.edu; Clifford E. Berkman, Washington State University, Department of Chemistry, Pullman, WA 99164-4630, cberkman@wsu.edu.

AUTHORS' CONTRIBUTIONS

F.P. Olatunji: Conceptualization, synthesis design, methodology, investigation, data curation, formal analysis, writing-original draft, writing-review and editing. **M. Pun:** Synthesis design, data curation, methodology. **J.W. Herman:** Synthesis and characterization. **O. Romero:** Synthesis and characterization. **M. Maniatopoulos:** PSMA IC50, methodology. **J.D. Latoche:** Efficacy and toxicity study, data curation, formal analysis. **R.A. Parise:** Biodistribution study, data curation, methodology. **J. Guo:** Biodistribution study, data curation, methodology. **J.H. Beumer:** Biodistribution study, data curation, formal analysis, supervision, funding acquisition, writing-review and editing. **C.J. Anderson:** Conceptualization, formal analysis, supervision, funding acquisition, methodology, project administration, writing-review and editing. **C.E. Berkman:** Conceptualization, formal analysis, supervision, funding acquisition, methodology, project administration, writing-review and editing.

Supporting Information for this article are available at Molecular Cancer Therapeutics Online (http://mct.aacrjournals.org).

Conflict of Interest Statement: none of the authors hold any competing interests.

MMAE was observed predominantly in tumor tissue, at levels that were 2-3 orders of magnitude higher than non-target tissues. Furthermore, SMDC**2**, which incorporated a novel pH-responsive phosporamidate linker, demonstrated significantly improved efficacy over SMDC**1** that has a valine-citrulline linker, with a 100% survival over 90 days and 4 out of 8 mice showing complete tumor growth inhibition after 6 weekly doses of 0.8 mg/kg (244 nmol/kg). Our findings demonstrate the potential of irreversible PSMA inhibitors combined with pH-responsive linkers as a way to specifically deliver chemotherapeutic drugs to PCa tumors with minimal toxicity.

INTRODUCTION

Prostate cancer (PCa) is the most diagnosed cancer in American men and one of the major causes of cancer-related deaths, second only to lung cancers.[1] Generally, patients with localized disease can be treated with radical prostatectomy and/or radiation therapy.[2] Patients with metastatic PCa can be temporarily treated with androgen deprivation strategies;[3] however, many progress to metastatic disease, which can evolve into castration-resistant cancer that does not respond to androgen deprivation therapy (mCRPC). Only 26-30% of patients with mCRPC survive 5 years.[1,4,5] Chemotherapy (e.g., docetaxel, cabazitaxel) is the standard treatment given following anti-androgen therapy failure, which often results in marginal responses accompanied by off-target toxicity.[6-8] Improved therapeutic approaches are critically needed for late-stage PCa patients that both improve efficacy and minimize toxicity.

Prostate-specific membrane antigen (PSMA) is a type II transmembrane protein that is highly overexpressed in the majority of all prostate cancers.[9,10] PSMA expression is more highly upregulated in poorly differentiated, metastatic, hormone-refractory carcinomas, and in cancer cells from mCRPC patients.[9-13] Furthermore, PSMA is constitutively internalized from the cell surface[14,15] making it an ideal target for imaging and therapy. Indeed, PSMA-targeted radiopharmaceutical therapies have shown considerable promise in clinical trials,[16-19] with ^{177}Lu-PSMA-617 recently receiving FDA breakthrough therapy designation.[20] Several other PSMA-targeted radioligand therapies and antibody-drug conjugate (ADCs)[21-24] have also demonstrated promising efficacy in preclinical studies. However, problems associated with relapse, off-target toxicity, immunogenicity of antibody-based therapies, and the stringent requirements imposed on the facilities that produce and manage radiopharmaceutical production represent significant challenges for drug development, FDA-approval, and use in the oncology community for these classes of agents to treat mCRPC.

Small molecule-drug conjugates (SMDCs) represent an attractive smart molecule alternative to the more conventional ADC approach for PSMA-targeted chemotherapeutic delivery.[25-27] Both technologies typically include a PSMA-targeting motif (antibody vs small-molecule enzyme inhibitor), a spacer, a cleavable linker, a potent cytotoxic payload and an albumin binder (in the case of SMDCs). After binding to cell-surface PSMA, these agents are expected to internalize and accumulate in endosomes and lysosomes, which enables efficient release of the cytotoxic payload in the target cells, typically by enzymatic cleavage.[28-31] Compared to anti-PSMA antibodies, small-molecule PSMA inhibitors exhibit comparable

accurate localization to the prostate cancer lesions; however, the considerably lower molecular weight and simpler molecular characterization will be associated with lower manufacturing costs, flexibility in determining the optimal dose regimen, and higher tolerated doses.[32-34] Importantly, the toxicity profile of PSMA-SMDCs should be much lower than ADCs, as they have a shorter residence time and undergo more rapid and uniform diffusion into the tumor mass compared to normal organs such as kidneys, lacrimal glands, and salivary glands.[33,34] In this proof-of-concept study, we describe the design, efficacy and pharmacokinetics of two novel PSMA-targeted SMDCs for treatment of mCRPC in mouse model (Figure 1).

MATERIALS AND METHODS

SMDC Synthesis and Characterization.

All starting materials and reagents were of commercial quality and were used without further purification. All anhydrous solvents used in reactions were obtained from commercial sources or freshly distilled over calcium hydride. ^{1}H, ^{13}C, and ^{31}P NMR spectra were recorded on a Varian 400, Brucker Avance Neo 500, or Varian 600 MHz spectrometer. ^{1}H NMR chemical shifts are relative to $CDCl_3$ (δ = 7.26 ppm), CD_3OD (δ = 3.31 ppm) or D_2O (δ = 4.79 ppm). ^{13}C NMR chemical shifts were relative to $CDCl_3$ (δ = 77.23 ppm) or CD_3OD (δ = 49.15 ppm). High-resolution mass spectrometry (HRMS) spectra were obtained on an Applied Biosystems 4800 MALDI-TOF/TOF mass spectrometer (Applied Biosystems, Foster City, CA). **CTT1700** (Figure 1) was obtained from Cancer Targeted Technology. The synthesis of SMDCs **1** and **2** is outlined in Figure 2. The synthesis of azides **10** and **11** are outlined in the Supporting Information and from a previously published study, respectively.[35]

***Methyl N2-((S)-5-(tert-butoxy)-2-((tert-butoxycarbonyl)amino)-5-oxopentanoyl)-N6-(4-(4-iodo phenyl) butanoyl)-D-lysinate* (5).—**A solution of acid, **4** (2 g, 6.59 mmol) and HBTU (2.5 g, 6.59 mmol) was stirred in anhydrous DMF (11 mL) under Ar at room temperature for 30 min. A solution of **3** (2.6 g, 7.91 mmol) and anhydrous Et_3N (2.5 mL, 16.5 mmol) in DMF (11 mL) was added to the reaction solution, and the reaction was stirred for 3 h under Ar. The reaction was diluted with EtOAc (150 mL) and washed sequentially with 1 N HCl (75 mL, 3x), sat. $NaHCO_3$ (aq) (75 mL, 2x) and Brine (75 mL, 1x). Organic layer was dried on Na_2SO_4, volatiles were removed under reduced pressure, resulting residue was dried under high vacuum and carried on to the next step without further purification. Isolated yield was 93%. ^{1}H NMR (400 MHz, DMSO-d_6) δ 8.14 (d, *J* = 7.7 Hz, 1H), 7.40 – 7.28 (m, 5H), 7.23 (t, *J* = 5.7 Hz, 1H), 6.82 (d, *J* = 8.3 Hz, 1H), 4.99 (s, 2H), 4.24 – 4.14 (m, 1H), 4.03 – 3.92 (m, 1H), 3.61 (s, 3H), 2.95 (q, *J* = 6.5 Hz, 2H), 2.20 (q, *J* = 6.6, 5.1 Hz, 2H), 1.81 (dq, *J* = 13.4, 6.8 Hz, 1H), 1.67 (m, 3H), 1.38(2s, 18H), 1.30 – 1.20 (m, 2H). ^{13}C NMR (126 MHz, Chloroform-d) δ 172.9, 172.6, 171.7, 156.6, 155.8, 136.7, 128.6, 128.5, 128.2, 128.1, 81.1, 80.2, 66.7, 54.3, 52.5, 51.9, 40.6, 39.4, 31.9, 31.8, 28.6, 28.3, 28.2, 27.3, 22.3, 21.2. HRMS (MALDI): m/z calculated for $C_{29}H_{45}KN_3O_9^+$ $[M+K]^+$: 618.27930, found 618.27661.

***(S)-4-carboxy-1-(((R)-6-(4-(4-iodophenyl)butanamido)-1-methoxy-1-oxohexan-2-yl)amino)-1-oxobutan-2-aminium chloride* (6).—**An evacuated flask containing **5** (3.4 g, 5.86 mmol) and Pd/C (0.34 g, 10% mass eq) in MeOH (60 mL) was charged with H_2 under balloon pressure. The reaction was stirred continuously until complete by TLC. Pd/C was filtered off using a celite pad, filtrate was concentrated under reduced pressure, the leftover residue was dried under high vacuum and carried on to the next step without further purification. A solution of 4-(4-iodophenyl)butanoic acid (1.7 g, 5.86 mmol) and HBTU (2.23 g, 5.86 mmol) was stirred in anhydrous DMF (10 mL) under Ar at room temperature for 30 min. A solution of Cbz-deprotected amine (2.74 g, 6.15 mmol) and anhydrous Et_3N (1.53 mL, 8.79 mmol) in DMF (10 mL) was added to the reaction solution, and the reaction was stirred for 6 h under Ar. The reaction was diluted with EtOAc (150 mL) and washed sequentially with 1N HCl (75 mL, 3x), sat. $NaHCO_3$ (aq) (75 mL, 2x) and brine (75 mL, 1x). The organic layer was dried on Na_2SO_4, volatiles were removed under reduced pressure, resulting residue was dried under high vacuum and carried on to the next step without further purification. Isolated yield of **Pre-6** was 85%. ^{1}H NMR (400 MHz, DMSO-d_6) δ 8.13 (d, J = 7.7 Hz, 1H), 7.74 (t, J = 5.6 Hz, 1H), 7.62 (d, J = 8.2 Hz, 2H), 7.00 (d, J = 8.2 Hz, 2H), 6.82 (d, J = 8.3 Hz, 1H), 4.19 (td, J = 8.5, 5.2 Hz, 1H), 3.99 (dt, J = 22.0, 7.6 Hz, 1H), 3.60 (s, 3H), 2.98 (hept, J = 6.3 Hz, 2H), 2.19 (q, J = 6.8, 6.1 Hz, 2H), 2.03 (t, J = 7.4 Hz, 2H), 1.69 (m, 5H), 1.38 (2s, 18H), 1.24 (q, J = 7.0 Hz, 2H). ^{13}C NMR (126 MHz, Chloroform-d) δ 173.33, 173.03, 172.57, 171.68, 155.86, 141.32, 137.46, 130.73, 91.06, 81.21, 80.33, 54.72, 52.59, 51.75, 39.13, 35.60, 34.82, 31.97, 31.83, 28.55, 28.37, 28.31, 28.16, 27.07, 22.28. HRMS (MALDI): m/z calculated for $C_{31}H_{48}IN_3NaO_8^+$ $[M+Na]^+$: 740.23783, found 740.24152. In a dry evacuated flask, a solution of Boc-protected amine **Pre-6** (0.099 g, 0.137 mmol) was stirred continuous in 4N HCl-1,4-dioxane (1 mL) for 1 h at room temperature. Volatiles were removed via rotary evaporation; the resulting residue was dried under high vacuum to yield an off-white solid in quantitative yield. ^{1}H NMR (400 MHz, DMSO-d_6) δ 8.95 (d, J = 7.5 Hz, 1H), 8.23 (d, J = 5.3 Hz, 3H), 7.79 (t, J = 5.6 Hz, 1H), 7.64 – 7.56 (m, 2H), 7.02 – 6.95 (m, 2H), 4.23 (q, J = 7.7 Hz, 1H), 3.85 (d, J = 5.8 Hz, 1H), 3.61 (s, 3H), 3.02 – 2.93 (m, 2H), 2.30 (h, J = 10.2, 9.7 Hz, 2H), 1.99 (dt, J = 19.2, 7.0 Hz, 4H), 1.69 (dp, J = 28.2, 7.5 Hz, 4H), 1.34 (q, J = 7.0 Hz, 2H), 1.25 (d, J = 8.0 Hz, 2H). ^{13}C NMR (126 MHz, DMSO-d_6) δ 173.3, 172.1, 171.7, 168.4, 141.7, 137.0, 130.9, 91.4, 66.4, 52.3, 52.0, 51.5, 38.0, 34.7, 34.1, 30.4, 29.2, 28.6, 26.9, 26.5, 22.7. HRMS (MALDI): m/z calculated for $C_{22}H_{34}ClIN_3O_6^+$ $[M+H]^+$: 598.14160, found 598.14044; m/z calculated for $C_{22}H_{33}ClIN_3NaO_6^+$ $[M+Na]^+$: 620.12361, found 620.12140.

***Compound* 7.—**To a stirring of solution of **6** (0.184 g. 0.308 mmol) and $NaHCO_3$ (0.0801 g, 0.800 mmol) in ddH_2O (2 mL) was added a solution of DBCO-PEG_4-NHS (0.1 g, 0.154 mmol) in 1,4-dioxane (2 mL) dropwise. The reaction was stirred at ambient temperature for 3 h. ddH_2O (10 mL) was added to the reaction solution and the pH was slowly adjusted to 2 via 1 N HCl. More ddH_2O (10 mL) was added, and the organics were extracted into EtOAc (20 mL, 3x). Organic layer was combined and dried under Na_2SO_4, followed by removal of solvent under reduced pressure and the resulting residue was purified via silica-gel flash chromatography (14% MeOH in CH_2Cl_2 → 20% MeOH in CH_2Cl_2) to yield a yellow solid in 70% yield. TLC: Rf = 0.194 (15% MeOH in CH_2Cl_2, visualization by UV). ^{1}H NMR (600 MHz, CD_3OD) δ 7.62 (dd, J = 7.6, 1.4 Hz, 1H), 7.58 – 7.52 (m, 2H), 7.45 (m, 1H),

7.43 – 7.38 (m, 2H), 7.31 (m, 2H), 7.22 (dd, J = 7.5, 1.5 Hz, 1H), 6.97 – 6.92 (m, 2H), 5.09 (d, J = 14.0 Hz, 1H), 4.40 (m, 1H), 4.35 (m, 1H), 3.70 – 3.61 (m, 6H), 3.61 – 3.46 (m, 13H), 3.25 – 3.19 (m, 1H), 3.17 – 3.04 (m, 3H), 2.56 – 2.38 (m, 5H), 2.32 (td, J = 7.3, 3.6 Hz, 2H), 2.30 – 2.25 (m, 2H), 2.14 (t, J = 7.5 Hz, 2H), 2.02 (ddt, J = 23.2, 16.0, 7.0 Hz, 2H), 1.92 – 1.76 (m, 4H), 1.71 – 1.62 (m, 1H), 1.44 (dp, J = 19.9, 6.6 Hz, 2H), 1.32 (m, 2H). ^{13}C NMR (151 MHz, CD_3OD) δ 175.6, 174.1, 173.9, 173.8, 173.1, 152.5, 149.5, 142.8, 138.5, 133.5, 131.8, 130.5, 130.0, 129.7, 129.2, 128.9, 128.1, 126.5, 124.3, 123.4, 115.6, 108.7, 91.5, 71.1, 70.9, 68.3, 68.1, 56.56, 54.1, 53.6, 52.8, 49.9, 39.9, 37.2, 37.1, 36.6, 36.3, 35.7, 35.4, 32.1, 32.0, 29.8, 29.7, 28.9, 28.5, 24.2. HRMS (MALDI): m/z calculated for $C_{52}H_{66}IN_5NaO_{13}^+$ $[M+Na]^+$: 1118.35940, found 1118.36194; m/z calculated for $C_{52}H_{66}IKN_5O_{13}^+$ $[M+K]^+$: 1134.33334, found 1134.33423.

***Compound* 8.—**To a stirring of solution of **7** (0.35 g, 0.319 mmol) and DIPEA (0.068 mL, 0.383 mmol) in anhydrous DMF (6 mL) was added TSTU (0.096 g, 0.319 mmol) in one portion under Argon. The reaction was stirred at ambient temperature for 3 h. A solution of CTT1298 (0.322 g, 0.415 mmol) and $KHCO_3$ (0.064 g, 0.639 mmol) in ddH_2O (4 mL) was added to the reaction solution and the reaction was stirred continuously overnight. Volatiles were removed under reduced pressure resulting residue was purified via reverse-phase flash chromatography (100% H_2O → 100% MeOH) to yield a yellow solid in 51% yield. TLC: Rf = 0.37 (70% MeOH in H_2O, visualization by UV). ^{1}H NMR (600 MHz, Deuterium Oxide) δ 7.69 (d, J = 7.6 Hz, 1H), 7.63 (d, J = 7.9 Hz, 2H), 7.55 – 7.41 (m, 6H), 7.37 (d, J = 7.6 Hz, 1H), 6.99 (d, J = 8.0 Hz, 2H), 5.09 (d, J = 14.3 Hz, 1H), 4.37 (dd, J = 9.4, 4.9 Hz, 1H), 4.33 – 4.27 (m, 1H), 4.15 (dd, J = 8.7, 4.7 Hz, 1H), 4.10 (dd, J = 8.3, 4.9 Hz, 1H), 3.80 – 3.55 (m, 26H), 3.54 – 3.47 (m, 1H), 3.20 (dt, J = 12.3, 5.7 Hz, 1H), 3.10 (dq, J = 28.9, 7.0 Hz, 6H), 2.82 (d, J = 1.0 Hz, 1H), 2.56 (m, 4H), 2.50 – 2.16 (m, 17H), 2.16 – 2.02 (m, 3H), 1.87 (m, 10H), 1.72 (m, 3H), 1.65 – 1.53 (m, 5H), 1.48 (m, 5H), 1.38 – 1.24 (m, 5H). ^{31}P NMR (234 MHz, Deuterium Oxide) δ 7.32. ^{13}C NMR (126 MHz, Deuterium Oxide) δ 183.9, 182.5, 182.4, 180.2, 179.3, 177.2, 175.9, 175.7, 175.2, 174.7, 174.6, 174.3, 174.0, 173.3, 151.6, 148.7, 142.5, 138.2, 133.2, 131.7, 130.2, 129.7, 129.5, 129.0, 127.9, 126.5, 123.6, 122.6, 115.7, 109.1, 92.3, 70.7, 70.6, 70.6, 70.6, 70.5, 67.8, 67.6, 65.4, 65.3, 57.6, 56.4, 55.8, 54.3, 53.7, 53.5, 40.3, 39.9, 39.7, 36.9, 36.8, 36.6, 36.5, 36.4, 35.3, 34.9, 34.8, 33.4, 33.1, 33.0, 32.9, 31.1, 29.2, 29.1, 29.0, 28.3, 28.1, 27.9, 27.8, 26.8, 25.9, 25.8, 23.6. HRMS (MALDI): m/z calculated for $C_{73}H_{101}IKN_9O_{25}P^+$ $[M+K]^+$: 1700.53225, found 1700.53699.

***Compound* 9.—**To a stirring of solution of **8** (0.29 g, 0.157 mmol) in ddH_2O (5 mL) was added 1 N KOH dropwise until the pH = 12.5. Reaction was stirred until completion by TLC. Reaction solution lyophilized to give an off-white solid and carried on to the next step without further purification. Isolated yield was quantitative. TLC: Rf = 0.42 (70% MeOH in H_2O, visualization by UV). ^{1}H NMR (600 MHz, Deuterium Oxide) δ 7.25 (d, J = 8.1 Hz, 2H), 7.23 – 7.06 (m, 6H), 6.65 (d, J = 8.0 Hz, 2H), 3.99 (tdd, J = 22.0, 8.6, 4.8 Hz, 4H), 3.65 – 3.53 (m, 5H), 3.48 – 3.24 (m, 19H), 3.03 – 2.83 (m, 7H), 2.42 (tt, J = 11.9, 7.6 Hz, 2H), 2.31 – 2.02 (m, 16H), 1.98 (t, J = 7.6 Hz, 5H), 1.86 – 1.63 (m, 8H), 1.62 – 1.40 (m, 10H), 1.32 (m,, 5H), 1.16 (m, 5H). ^{31}P NMR (234 MHz, Deuterium Oxide) δ 7.35. ^{13}C NMR (151 MHz, Deuterium Oxide) δ 183.1, 181.5, 181.4, 179.3, 178.5, 176.4, 175.0, 174.5, 173.8,

173.1, 172.7, 172.5, 150.5, 147.6, 141.5, 137.1, 132.2, 130.7, 129.2, 128.7, 128.5, 128.1, 126.9, 125.5, 122.5, 121.6, 114.7, 108.1, 91.4, 69.6, 69.5, 69.4, 66.7, 66.6, 64.4, 64.3, 56.5, 55.4, 54.9, 53.8, 39.3, 39.2, 38.7, 35.8, 35.7, 35.5, 35.4, 35.3, 34.3, 33.8, 33.7, 32.3, 32.1, 32.0, 31.9, 31.3, 28.2, 28.0, 27.8, 27.2, 27.0, 26.8, 26.7, 24.9, 24.8, 22.7. HRMS (MALDI): m/z calculated for $C_{72}H_{98}IKN_9O_{25}P^+$ $[M+K]^+$: 1685.51729, found 1685.51514.

***SMDC* 1.—**A solution of **10** (48 mg, 30.5 μmol) in (2 mL) was added a solution of **9** (50 mg, 32.5 μmol) in ddH_2O (2 mL); the reaction was stirred for 30 min at ambient temperature. Solvent was removed under reduced pressure and the resulting residue was purified by RP-Prep HPLC (5% CH_3CN in 10mM NH_4OAc → 100% CH_3CN, gradient shown in Supporting Information). Fractions containing the desired product were combined, the NH_4OAc was neutralized with excess $KHCO_3$ (approx. 2 eq), solvents were removed under reduced pressure and the resulting residue was lyophilized overnight. The solids were desalted using a C18 Sep-Pak (100% ddH_2O → 100% MeOH) to yield an off-white solid product in 30%. ^{31}P NMR (234 MHz, Deuterium Oxide) δ 7.41. HRMS (ESI-MS): m/z calculated for $C_{138}H_{196}IN_{22}O_{38}P^{2-}/2$ $[M-2H]^{2-}/2$: 1463.6432, found 1463.6420; m/z calculated for $C_{138}H_{196}IN_{22}O_{38}P^{3-}/3$ $[M-3H]^{3-}/3$: 975.4262, found 975.4267; m/z calculated for $C_{138}H_{196}IN_{22}O_{38}P^{4-}/4$ $[M-4H]^{4-}/4$: 731.3177, found 731.3133.

***SMDC* 2.—**Following the synthesis and purification of **1** above, **9** (50 mg, 27.0 μmol), **11** (41 mg, 29.7 μmol) and ddH_2O (4 mL) were used. Isolated yield was 49%.^{31}P NMR (234 MHz, Deuterium Oxide) δ 9.59, 9.35, 7.42. HRMS (ESI-MS): m/z calculated for $C_{138}H_{193}IN_{20}O_{42}P_2^{2-}/2$ $[M-2H]+^{-}/2$: 1483.6051, found 1483.6007, found 1463.6420; m/z calculated for $C_{138}H_{193}IN_{20}O_{42}P_2^{3-}/3$ $[M-3H]^{3-}/3$: 988.7341, found 988.7234, found 975.4267; m/z calculated for $C_{138}H_{193}IN_{20}O_{42}P_2^{4-}/4$ $[M-4H]^{4-}/4$: 741.2986, found 741.2957.

Pharmacokinetics

In vivo experiments were conducted according to Institutional Animal Care and Use Committee Policy. All animal studies were also approved and supervised by the University of Pittsburgh Institutional Animal Care and Use Committee in accordance with the Animal Welfare Act, the Guide for the Care and Use of Laboratory Animals and NIH guidelines. NCr nude mice (age 6-8 weeks) were injected subcutaneously with $1x10^6$ PC3-PiP cells (100 μL, 1:1 saline/Matrigel). When tumors reached a size of approximately 100 mm^3, 3 groups of 4 mice per drug were injected IV (lateral tail vein) with a single dose of 0.8 mg/kg of the respective drug formulated in PBS (10 μL/g). At 1 and 6 h post-dose, blood (retroorbital) was collected from groups of 4 mice. At approximately 24, 72, and 120 h, groups of 4 mice were euthanized, and blood was collected by cardiac puncture with EDTA flushed syringes, and plasma was isolated by centrifugation at 12,000 x g for 4 min. Tumor, lacrimal gland, kidney, and prostate were obtained from the mice, and weighed, snap frozen in liquid N_2 and stored at −80°C until homogenization. Plasma and homogenized tissue samples were analyzed via LC-MS/MS for SMDC and MMAE content. Three volumes of PBS, pH 7.4, were added to tumor, kidney, and lacrimal tissues and 10 volumes of PBS, pH 7.4, were added to prostate tissue samples. Tumor, kidney, and prostate samples were homogenized with a homogenizer, and lacrimal tissues were sonicated with a sonicator.

Twenty five microliters of plasma or tissue homogenate was added to a microcentrifuge tube followed by 10 μL of internal standard solution and 100 μL of 5 mM ammonium bicarbonate and acetonitrile (25:75 *v,v*). The sample was then vortexed at a high setting for 1 minute and centrifuged at 17,200 x g for 10 minutes. The resultant supernatant was pipetted into an HPLC vial and 10-20 μL was injected into the LC-MS/MS system. SMDC **2** was used as internal standard for the quantitation of CTT1700 and SMDC **1**, and SMDC **1** was used as internal standard for SMDC **2**. [$^2H_8$]-MMAE was used as the internal standard for MMAE. CTT1700 (MW 3013.4 g/mol), **2** (MW 3275.7 g/mol) and **1** (MW 3159.6 g/mol) concentrations were quantitated using a SCIEX (Framingham, MA 01701) 4500 LC-MS/MS system consisting of an Exion HPLC and 4500 mass detector. A SCIEX 6500+ Qtrap LC-MS/MS system consisting of an Agilent (Palo Alto, CA 94036) 1290 HPLC and Sciex 6500+ QTrap mass detector was used for quantitation of MMAE concentrations. The chromatography consisted of a gradient using of 5 mM ammonium bicarbonate and acetonitrile and the separation was achieved using a Phenomenex (Torrance, CA 90501) Kinetex column (2 x 50 mm, 2.6 μm). The MRM *m/z* transitions monitored were 903.1/419.0, 990.7/419.0, 977.8/718.4, 718.5/686.5 and 726.5/694.5 for CTT1700, **2**, **1**, MMAE and [$^2H_8$]-MMAE, respectively. Standard curves were linear from 10-10,000 ng/mL for CTT1700, **2** and **1** while the MMAE standard curves were linear from 0.01 to 10 ng/mL. A $1/y^2$ weighted linear regression was used for all standard curves. PK parameters were estimated using standard noncompartmental methods with Phoenix WinNonlin (Certara, Princeton, NJ). Plasma parent drugs were derived using the IV bolus approach, while all other data were derived using the extravascular approach.

In-vivo efficacy

To evaluate efficacy of SMDCs **1** and **2** in a mouse model of human PCa, we employed PSMA+ PC3-PIP tumor cells implanted subcutaneously in the right rear flank of NCr nude mice (6 – 8 weeks old). Three weeks after injection of the cells, when the tumor volume reached an average tumor size of ~130 mm^3, mice were treated with 0.8 mg/kg of each SMDC (253 nmol/kg of SMDC **1**; 244 nmol/kg of SMDC **2**; 265 nmol/kg of CTT1700; n = 8 for each SMDC) via lateral tail vein injection (100 μL bolus) once weekly for six weeks. Tumor sizes were measured twice weekly for the duration of the study and mice were monitored for 90 days after first administration. Mice were euthanized if the tumor size or mouse health reached IACUC standards for euthanasia (tumor burden of >1.5 cm in any axis, ulceration, >20% mouse weight loss). Blood draws were taken via superficial temporal vein at 0, 4, 7 and 10 weeks, and complete blood count (CBC) analysis was performed with a 3-part differential measurement.

Data Availability

The data generated in this study are available within the article and its supplementary data files.

RESULTS

SMDC Synthesis

The synthesis of SMDCs **1** and **2** were achieved through copper-free click reactions (Figure 2). The key common precursor to both **1** and **2** is compound **9**, which contains the strained dibenzocyclooctyne for click chemistry, CTT1298 as the targeting molecule, and the albumin-binding moiety into its molecular structure. Azides **10** and **11** incorporate the Val-Cit and phosphoramidate linkers, respectively, in addition to the cytotoxic payload. The click-chemistry reactions were monitored by HPLC and found to be complete in less than 30 minutes. SMDCs **1** and **2** were purified by preparative C18-HPLC and further desalted to give isolated yields of 30% and 49%, respectively; they were fully characterized by HRMS, HPLC and ^{31}P NMR (see Supporting Information). Once characterized, IC_{50} values for PSMA binding were determined as described previously and found to be in the nanomolar range for **1** (IC_{50} = 37.9 ± 7.5 nM) and **2** (IC_{50} = 1.67 ± 0.14 nM), consistent with other PSMA inhibitors of this class. CTT1700 was generously provided by Cancer Targeted Technology.

Pharmacokinetic studies

Plasma and tumor levels of parent compounds SMDC **1**, SMDC **2**, and CTT1700, along with released MMAE are shown in Figure 3 and Table S1. The plasma levels of SMDCs and released MMAE give an indication of overall exposure, while the levels in the kidneys and lacrimal gland (see Figure 4) represent the off-target organs typically affected negatively by PSMA-targeted agents.[36] Parent SMDCs **1** and **2** exhibited a distribution volume of 0.106 and 0.122 L/kg, respectively, a value in between plasma volume and extracellular water volume . This is indicative of the albumin binding motif enhancing half-life and retention of the SMDCs in plasma. Released MMAE was undetectable in the plasma of mice administered with compound **1**, likely due to the more rapid clearance of this compound compared to CTT1700 and **2** (Figure 3A, B, and C). In the tumor, the concentration of MMAE released from **2** increased between days 3 and 5, whereas MMAE from **1** leveled off at 3 days (Figure 3E and F). CTT1700, which employs a linker that slowly releases MMAE, reaches a concentration in the tumor that is approximately 5-fold lower than that of **1** or **2** (Figure 3D). MMAE concentrations upon release from CTT1700, **1** and **2** were comparable in prostate, kidneys, and lacrimal glands and were all 2-3 orders of magnitude lower than that in the tumor (Figure 4A-I).

In addition, we investigated the stabilities of all three SMDCs in mouse plasma at 37°C for 24 h (see Figure S1). No degradation was observed for CTT1700 and SMDC **2**. In sharp contrast, SMDC **2** showed rapid degradation following apparent first-order kinetics with a half-life of 3.5 h and approximately 60% of associated MMAE released was observed over 24 h.

In-vivo efficacy.

Tumor growth and survival data for mice administered with controls and SMDCs **1** and **2** are shown in Figure 5 and S2. Animals in the saline and MMAE control groups reached tumor size end point criteria within 6 weeks of their first administration (Figure 5A, B).

This was expected for MMAE administration, since the cytotoxic agent is known to be non-specific, with minimal accumulation in the tumor. Animals that were treated with CTT1700, a PSMA-targeted SMDC with a slowly cleavable phosphoramidate linker due to steric congestion around the labile P-N bond, showed moderate efficacy, with all animals reaching end point tumor burden within 12 weeks of dosing initiation (Figure 5C). In sharp contrast, SMDCs **1** and **2** showed considerable efficacy compared to the saline and MMAE controls (SMDC **1**: $p < 0.02$, SMDC **2**: $p < 0.0001$). For animals treated with SMDC **1**, tumor regression was observed following initiation of administration up until 2 weeks after the last dose, with subsequent tumor growth in five of the eight mice. Five of eight mice survived 90 days after initial dosing (Figure 5D). Animals treated with SMDC **2** showed durable tumor growth regression, with no detectable tumor in any of the mice by day 35 of first dosage (Figure 3E), and growth in four of seven mice commencing five weeks after the last drug administration. The survival of mice in the SMDC **2** group were statistically greater than the other groups, including SMDC **1** ($p < 0.0001$), with all animals surviving at 90 days (Figure 3F). It is important to note that in all groups of mice, body weights were stable or increased over the duration of the study, there were no overt visual signs of toxicity (scruffy coat, diarrhea, lethargy), and complete blood count (CBC) results were all in the normal range (see Supporting Information, Figures S3-S15).

DISCUSSION

Herein, we describe the development of two PSMA-targeted SMDCs (**1** and **2**; Figure 1A), distinguishable by their cleavable linkers, and assessment of their *in vivo* pharmacokinetics and efficacy in mice bearing PSMA(+) tumor xenografts. Compound **1** contains a valine-citrulline (Val-Cit) dipeptide linker, which is currently a component of FDA-approved ADC drugs[37-41] (e.g., Adcetris® and Polivy®). This linker is cleavable by lysosome-abundant cathepsin B proteases to release the cytotoxic payload.[42] In compound **2**, we used a novel acid-labile phosphoramidate linker recently developed in our lab.[35,43] This linker exhibits stability at neutral pH in plasma, with rapid release of payloads under the acidic conditions of endosomal and lysosomal compartments. Monomethyl auristatin E (MMAE), an anti-tubulin agent that kills cells at sub-nanomolar concentrations by inhibiting the assembly of microtubules followed by subsequent induction of mitotic arrest, was used as the cytotoxic payload for both SMDCs. CTT1700, a compound provided by Cancer Targeted Technology, employs a linker that slowly releases MMAE.[44] The phosphoramidate-based inhibitor, CTT1298, was selected as the PSMA-targeting molecule based upon its documented high-affinity, irreversible binding to PSMA (IC_{50} = 19 nM) and high selectivity for PSMA-expressing cancer cells.[45] Once bound to extracellular PSMA, CTT1298 derivatized with radiolabeled pendant groups has been shown to undergo rapid and extensive internalization in PSMA-expressing tumor cells.[45] Moreover, conjugation of chemical moieties to CTT1298 does not diminish the binding affinity of this ligand to PSMA.[36,45]

One of the major pharmacokinetic challenges for many of the small-molecule PSMA inhibitors with respect to delivering therapeutic payloads is their rapid renal clearance. To overcome this,[46] we outfitted the two SMDCs with an albumin-binding motif[47] known to reduce blood clearance while increasing tumor uptake of drug-conjugates.[36,48] Generally,

the observed plasma MMAE and parent drug profiles exhibited parallel and roughly mono-exponential profiles. Furthermore, we observed drug-released MMAE elimination half-lives ($t_{1/2}$) from plasma of 13 h and 24 h for SMDC **1** and **2** respectively, much higher than the $t_{1/2}$ of 4.1 h reported for MMAE when dosed directly.[49] These observations are indicative of formation rate limited elimination, with the pharmacokinetics (PK) of the parent drug determining and prolonging MMAE exposure.

Plasma concentrations of the MMAE were found to be 5 orders of magnitude lower than the parent drugs indicating low systemic release of MMAE payload. In tumors, concentrations of the parent drugs (**1**, **2**, and CTT1700) were roughly in the same order of magnitude suggesting similar efficiency in targeting, while MMAE concentrations varied between compounds according to linker stability.

We observed the slow decline of CTT1700 and **2** in all tissues over the course of 5 days. Surprisingly, SMDC **1** could not be quantified in any other tissue other than the tumor. This anomaly can be partly attributed to the reported low hydrolytic stability of valine-citrulline linkers in mouse plasma[50,51] and the rapid clearance and distribution of released-MMAE to highly perfused tissues like the liver, heart, lungs, and spleen.[49] This is further corroborated by *in vitro* mouse plasma stability results that delineates the apparent lability of valine-citrulline linker in SMDC **1** compared to superior stability of the phosphoramidate linkers found in CTT1700 and SMDC **2**. MMAE concentrations in normal tissues appeared to remain constant or decline over time, while MMAE concentrations in tumor continue to show steady increase between days 1 and 5, for all SMDCs. This is indicative of the slow turnover and selective accumulation of MMAE from the parent SMDCs in the tumor tissue preferentially to the other tissues. Moreover, SMDCs **1** and **2** resulted in approximately 6-fold higher absolute tumor MMAE exposure compared to the SMDC with a slowly degradable linker, CTT1700.[52]

The reported plasma clearance of MMAE of 60 mL/h (corresponds to 47 L/d/kg), allows us to use the apparent MMAE formation clearance we observed in our data to calculate the fraction of parent compound that is converted to MMAE. The fraction of drug that is estimated to release MMAE for CTT1700, SMDCs 1 and 2 was 1%, 38%, and 36%, respectively. This 40-fold difference in MMAE-releasing ability between CTT1700 relative to **1** and **2** was reflected in MMAE tumor concentrations, arguably, the most important metric for interpreting our efficacy data.

Based on the efficacy data and CBC analyses (Figure S3-15), the dose regimen uniformly utilized for this comparative study is below the maximum tolerated dose (MTD) in immune-compromised nude mice. Other PSMA-targeted MMAE-loaded SMDCs with the Val-Cit linker have been reported in the literature and investigated in the PC3-PIP model.[11,52] Although direct comparisons are not possible as the doses and regimens are different, agents **1** and **2** compare favorably with lower[11] and fewer[52] doses to achieve tumor growth inhibition and survival out to 90 days. A highly significant finding is that SMDC **2**, with the pH sensitive linker, is more effective than SMDC **1** that has the Val-Cit linker similar to previously published PSMA-targeted SMDCs. In addition, the improved performance of

SMDC **2** could also, in part, be attributed to its 15-fold greater binding to PSMA compared to SMDC **1**.

In summary, the pharmacokinetics and properties of the pH-responsive linker in **2** can be correlated with its superior efficacy when compared to the more stable phosphoramidate linkage in CTT1700.[35] The data indicate that efficient release of the payload from **2** reflects an optimal design of its versatile acid-labile linker. In addition, the *in vivo* performance of SMDC **2** compared to that of SMDC **1** demonstrates that the acid-labile phosphoramidate linker produced significantly greater efficacy than the Val-Cit linker that is prevalent in ADCs and recently reported SMDCs[11,48]. Although the efficacy and biodistribution experiments conducted are proof-of-concept studies, the results obtained warrant further exploration of the novel acid-labile phosphoramidate linker technology in the context of the controlled release of other clinically relevant payloads, as well as additional rigorous preclinical studies prior to advancement into the clinic.

Supplementary Material

Refer to Web version on PubMed Central for supplementary material.

ACKNOWLEDGMENTS

This work and F.P.O were supported by the National Institutes of Health (R21CA256382, R50CA211241, P30CA47904 and T32GM8336). The authors extend their gratitude for technical assistance to Dr. William Hiscox (WSU Center for NMR Spectroscopy), Dr. Gerhard Munske (WSU Laboratory of Biotechnology and Bioanalysis), and Dr. Deobald Lee (Mass Spectrometry Core Laboratory at University of Idaho). The authors would like the thank Cancer Targeted Technology for providing CTT1700 and to Dr. Damilola Olabode from AstraZeneca for providing statistical assistance on the efficacy study.

REFERENCES

1. Cancer Facts & Figures 2022. https://cancerstatisticscenter.cancer.org/?_ga=2.183764260.348552489.1635625673-888385122.1627324223#!/.
2. Wilkins LJ, Tosoian JJ, Sundi D, Ross AE, Grimberg D, Klein EA, et al. Surgical management of high-risk, localized prostate cancer. Nat. Rev. Urol 17, 679–690 (2020).
3. Perera M, Roberts MJ, Klotz L, Higano CS, Papa N, Sengupta S, et al. Intermittent versus continuous androgen deprivation therapy for advanced prostate cancer. Nat. Rev. Urol. 2020 178 17, 469–481 (2020).
4. Cho S, Zammarchi F, Williams DG, Havenith CE, Monks NR, Tyrer P, et al. Antitumor Activity of MEDI3726 (ADCT-401), a Pyrrolobenzodiazepine Antibody–Drug Conjugate Targeting PSMA, in Preclinical Models of Prostate Cancer. Mol. Cancer Ther 17(10), 2176–2186 (2018).
5. Semenas J, Allegrucci C, Boorjian SA, Mongan NP & Persson J. Liao Overcoming Drug Resistance and Treating Advanced Prostate Cancer. Curr. Drug Targets 13, 1308–1323 (2012).
6. Mita AC, Figlin R & Mita MM Cabazitaxel: More Than a New Taxane for Metastatic Castrate-Resistant Prostate Cancer? Clin. Cancer Res 18, 6574–6579 (2012).
7. Cushen SJ, Power DG, Murphy KP, McDermott R, Griffin BT, Lim M, et al. Impact of body composition parameters on clinical outcomes in patients with metastatic castrate-resistant prostate cancer treated with docetaxel. Clin. Nutr. ESPEN 13, e39–e45 (2016).
8. Moussa M, Papatsoris A, Chakra MA, Sryropoulou D & Dellis A Pharmacotherapeutic strategies for castrate-resistant prostate cancer. Exp. Op. Pharm 21, 1431–1448 (2020).
9. Mannweiler S, Amersdorfer P, Trajanoski S, Terrett JA, King D and Mehes G Heterogeneity of Prostate-Specific Membrane Antigen (PSMA) Expression in Prostate Carcinoma with Distant Metastasis. Pathol. Oncol. Res. 2008 152 15, 167–172 (2008).

10. Silver DA, Pellicer I, Fair WR, Heston WD & Cordon-Cardo C Prostate-specific membrane antigen expression in normal and malignant human tissues. Clin. Cancer Res 3(1), 81–85 (1997).
11. Wang X, Shirke A, Walker E, Sun R, Ramamurthy G, Wang J et al. Small Molecule-Based Prodrug Targeting Prostate Specific Membrane Antigen for the Treatment of Prostate Cancer. Cancers 13(3), 417 (2021).
12. Bostwick DG, Pacelli A, Blute M, Roche P & Murphy GP Prostate Specific Membrane Antigen Expression in Prostatic Intraepithelial Neoplasia and Adenocarcinoma A Study of 184 Cases. Cancer: Interdisciplinary International Journal of the American Cancer Society 82, 11 (1998).
13. Wright GL Jr, Grob BM, Haley C, Grossman K, Newhall K, Petrylak D, et al. Upregulation of prostate-specific membrane antigen after androgen-deprivation therapy. Urology 48, 326–334 (1996).
14. Liu H, Rajasekaran AK, Moy P, Xia Y, Kim S, Navarro V, et al. Constitutive and Antibody-induced Internalization of Prostate-specific Membrane Antigen. Cancer Res. 58, (1998).
15. Begum NJ, Glatting G, Wester HJ, Eiber M, Beer AJ & Kletting P The effect of ligand amount, affinity and internalization on PSMA-targeted imaging and therapy: A simulation study using a PBPK model. Sci. Reports 2019 91 9, 1–8 (2019).
16. Behr SC, Aggarwal R, VanBrocklin HF, Flavell RR, Gao K, Small EJ, et al. Phase I Study of CTT1057, an 18F-Labeled Imaging Agent with Phosphoramidate Core Targeting Prostate-Specific Membrane Antigen in Prostate Cancer. J. Nucl. Med 60, 910–916 (2019).
17. Violet J, Sandhu S, Iravani A, Ferdinandus J, Thang SP, Kong G, et al. Long-Term Follow-up and Outcomes of Retreatment in an Expanded 50-Patient Single-Center Phase II Prospective Trial of 177Lu-PSMA-617 Theranostics in Metastatic Castration-Resistant Prostate Cancer. J. Nucl. Med 61, 857–865 (2020).
18. Miyahira AK, Pienta KJ, Babich JW, Bander NH, Calais J, Choyke P, et al. Meeting report from the Prostate Cancer Foundation PSMA theranostics state of the science meeting. Prostate 80, 1273–1296 (2020).
19. Rowe SP, Drzezga A, Neumaier B, Dietlein M, Gorin MA, Zalutsky MR et al. Prostate-Specific Membrane Antigen–Targeted Radiohalogenated PET and Therapeutic Agents for Prostate Cancer. J. Nucl. Med 57, 90S–96S (2016).
20. Novartis receives FDA Breakthrough Therapy designation for investigational 177Lu-PSMA-617 in patients with metastatic castration-resistant prostate cancer (mCRPC) | Novartis. https://www.novartis.com/news/novartis-receives-fda-breakthrough-therapy-designation-investigational-177lu-psma-617-patients-metastatic-castration-resistant-prostate-cancer-mcrpc. Published on Jun 16, 2021
21. Wang X, Ma D, Olson WC & Heston WDW In Vitro and In Vivo Responses of Advanced Prostate Tumors to PSMA ADC, an Auristatin-Conjugated Antibody to Prostate-Specific Membrane Antigen. Mol. Cancer Ther 10, 1728–1739 (2011).
22. Huang CT, Guo X, Bařinka C, Lupold SE, Pomper MG, Gabrielson K, et al. Development of 5D3-DM1: A Novel Anti-Prostate-Specific Membrane Antigen Antibody-Drug Conjugate for PSMA-Positive Prostate Cancer Therapy. Mol. Pharm 17, 3392–3402 (2020).
23. Petrylak DP, Kantoff P, Vogelzang NJ, Mega A, Fleming MT, Stephenson JJ Jr, et al. Phase 1 study of PSMA ADC, an antibody-drug conjugate targeting prostate-specific membrane antigen, in chemotherapy-refractory prostate cancer. Prostate 79, 604–613 (2019).
24. Sartor O, De Bono J, Chi KN, Fizazi K, Herrmann K, Rahbar K, et al. Lutetium-177–PSMA-617 for Metastatic Castration-Resistant Prostate Cancer. New Eng. J. Med 385, 1091–1103 (2021).
25. Krall N, Scheuermann J & Neri D Small Targeted Cytotoxics: Current State and Promises from DNA-Encoded Chemical Libraries. Angew. Chemie Int. Ed 52, 1384–1402 (2013).
26. Krall N, Pretto F, Decurtins W, Bernardes GJ, Supuran CT and Neri D A Small-Molecule Drug Conjugate for the Treatment of Carbonic Anhydrase IX Expressing Tumors. Angew. Chemie Int. Ed 53, 4231–4235 (2014).
27. Vlahov IR & Leamon CP Engineering Folate–Drug Conjugates to Target Cancer: From Chemistry to Clinic. Bioconjug. Chem 23, 1357–1369 (2012).
28. Bareford LM & Swaan PW Endocytic mechanisms for targeted drug delivery. Adv. Drug Deliv. Rev 59, 748–758 (2007).

29. Tumey LN An Overview of the Current ADC Discovery Landscape. Methods Mol. Biol 2078, 1–22 (2020).
30. Chalouni C & Doll S Fate of Antibody-Drug Conjugates in Cancer Cells. J. Exp. Clin. Cancer Res 37, 1–12 (2018).
31. Xu S Internalization, Trafficking, Intracellular Processing and Actions of Antibody-Drug Conjugates. Pharm. Res 32, 3577–3583 (2015).
32. Patel TK, Adhikari N, Amin SA, Biswas S, Jha T and Ghosh B Small molecule drug conjugates (SMDCs): an emerging strategy for anticancer drug design and discovery. New J. Chem 45, 5291–5321 (2021).
33. Casi G & Neri D Antibody–Drug Conjugates and Small Molecule–Drug Conjugates: Opportunities and Challenges for the Development of Selective Anticancer Cytotoxic Agents. J. Med. Chem 58, 8751–8761 (2015).
34. Zhuang C, Guan X, Ma H, Cong H, Zhang W and Miao Z Small molecule-drug conjugates: A novel strategy for cancer-targeted treatment. Eur. J. Med. Chem 163, 883–895 (2019).
35. Olatunji FP, Herman JW, Kesic BN, Olabode D & Berkman CE A click-ready pH-triggered phosphoramidate-based linker for controlled release of monomethyl auristatin E. Tetrahedron Lett. 61, (2020).
36. Choy CJ, Ling X, Geruntho JJ, Beyer SK, Latoche JD, Langton-Webster B, et al. 177Lu-labeled phosphoramidate-based PSMA inhibitors: The effect of an albumin binder on biodistribution and therapeutic efficacy in prostate tumor-bearing mice. Theranostics 7, 1928–1939 (2017).
37. Akaiwa M, Dugal-Tessier J & Mendelsohn BA Antibody–Drug Conjugate Payloads; Study of Auristatin Derivatives. Chem. Pharm. Bull 68, 201–211 (2020).
38. Yip V, Lee MV, Saad OM, Ma S, Khojasteh SC and Shen BQ Preclinical Characterization of the Distribution, Catabolism, and Elimination of a Polatuzumab Vedotin-Piiq (POLIVY®) Antibody–Drug Conjugate in Sprague Dawley Rats. J. Clin. Med 10, 1323 (2021).
39. Bargh JD, Isidro-Llobet Albert, Parker JS & Spring DR Cleavable linkers in antibody–drug conjugates. Chem. Soc. Rev 48, 4361–4374 (2019).
40. Beck A, Goetsch L, Dumontet C & Corvaïa N Strategies and challenges for the next generation of antibody–drug conjugates. Nat. Rev. Drug Discov 16, 315–337 (2017).
41. Scott LJ Brentuximab Vedotin: A Review in CD30-Positive Hodgkin Lymphoma. Drugs 77, (2017).
42. Doronina SO, Toki BE, Torgov MY, Mendelsohn BA, Cerveny CG, Chace DF, et al. Development of potent monoclonal antibody auristatin conjugates for cancer therapy. Nat. Biotechnol. 2003 217 21, 778–784 (2003).
43. Olatunji FP, Savoy EA, Panteah M, Mesbahi N, Abbasi A, Talley CM, et al. Prostate-Specific Membrane Antigen-Targeted Turn-on Probe for Imaging Cargo Release in Prostate Cancer Cells. Bioconjug. Chem 32, 2386–2396 (2021).
44. Abdollahpour-Alitappeh M, Lotfinia M, Bagheri N, Sineh Sepehr K, Habibi-Anbouhi M, Kobarfard F, et al. Trastuzumab-monomethyl auristatin E conjugate exhibits potent cytotoxic activity in vitro against HER2-positive human breast cancer. J. Cell. Physiol 234, 2693–2704 (2019).
45. Dannoon S, Ganguly T, Cahaya H, Geruntho JJ, Galliher MS, Beyer SK, et al. Structure–Activity Relationship of 18F-Labeled Phosphoramidate Peptidomimetic Prostate-Specific Membrane Antigen (PSMA)-Targeted Inhibitor Analogues for PET Imaging of Prostate Cancer. J. Med. Chem 59, 5684–5694 (2016).
46. Liu Zhibo & Chen Xiaoyuan. Simple bioconjugate chemistry serves great clinical advances: albumin as a versatile platform for diagnosis and precision therapy. Chem. Soc. Rev 45, 1432–1456 (2016).
47. Dumelin CE, Trüssel S, Buller F, Trachsel E, Bootz F, Zhang Y, et al. A Portable Albumin Binder from a DNA-Encoded Chemical Library. Angew. Chemie 120, 3240–3245 (2008).
48. Müller C, Struthers H, Winiger C, Zhernosekov K & Schibli R DOTA Conjugate with an Albumin-Binding Entity Enables the First Folic Acid–Targeted 177Lu-Radionuclide Tumor Therapy in Mice. J. Nucl. Med 54, 124–131 (2013).

49. Yang RS, Chang LW, Yang CS & Lin P Whole-Body Pharmacokinetics and Physiologically Based Pharmacokinetic Model for Monomethyl Auristatin E (MMAE). J. Clin. Med 10, 1332 (2021).

50. Dorywalska M, Dushin R, Moine L, Farias SE, Zhou D, Navaratnam T, et al. Molecular basis of valine-citrulline-PABC linker instability in site-specific ADCs and its mitigation by linker design. Mol. Cancer Ther 15, 958–970 (2016).

51. Anami Y, Yamazaki CM, Xiong W, Gui X, Zhang N, An Z, et al. Glutamic acid–valine–citrulline linkers ensure stability and efficacy of antibody–drug conjugates in mice. Nat. Commun. 2018 91 9, 1–9 (2018).

52. Boinapally S, Ahn HH, Cheng B, Brummet M, Nam H, Gabrielson KL, et al. A prostate-specific membrane antigen (PSMA)-targeted prodrug with a favorable in vivo toxicity profile. Sci. Reports 2021 111 11, 1–10 (2021).

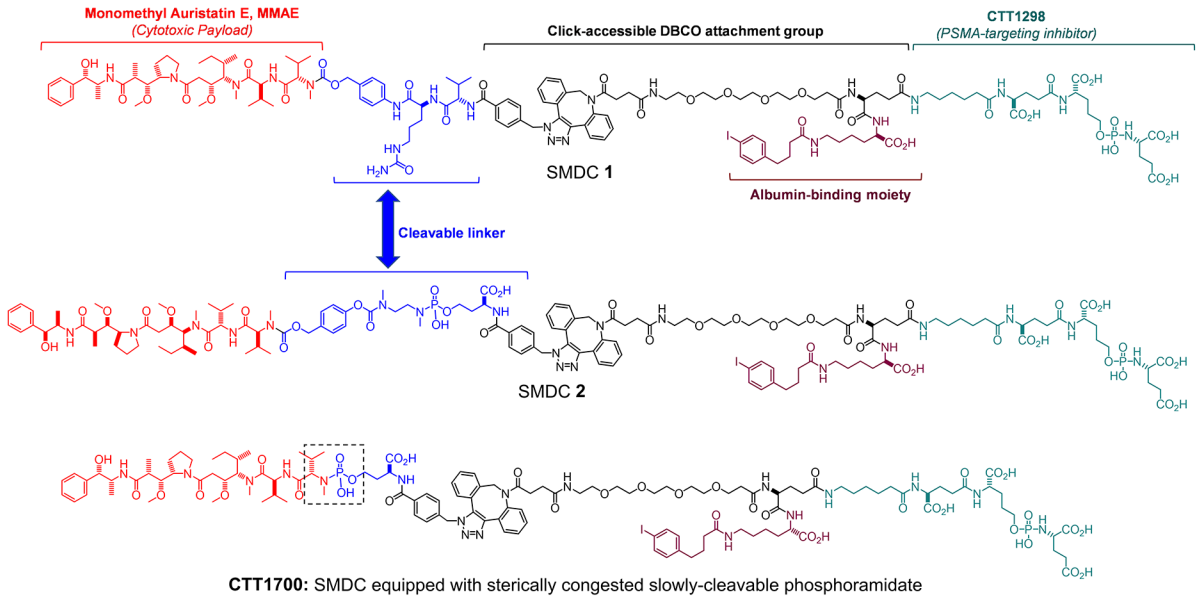

Figure 1:
SMDCs **1** (Val-Cit-SMDC), **2** (Phosphoramidate-SMDC), and **CTT1700**.

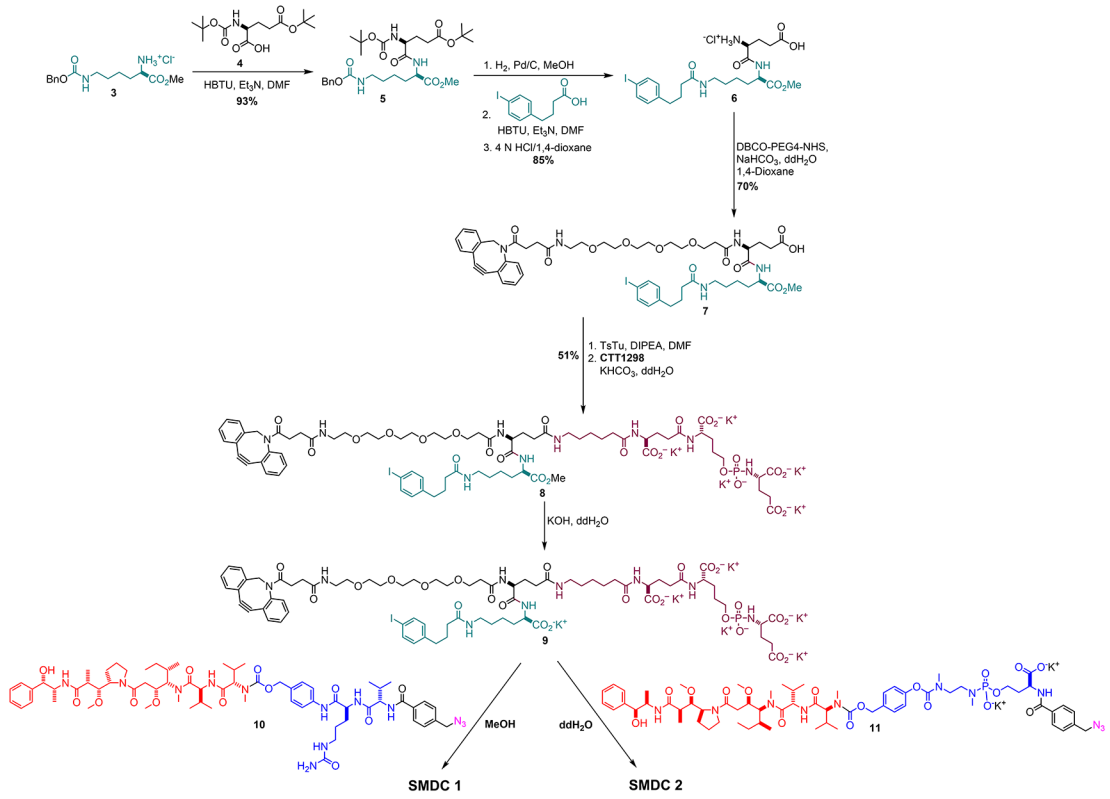

Figure 2:
Synthesis of SMDCs **1** and **2**.

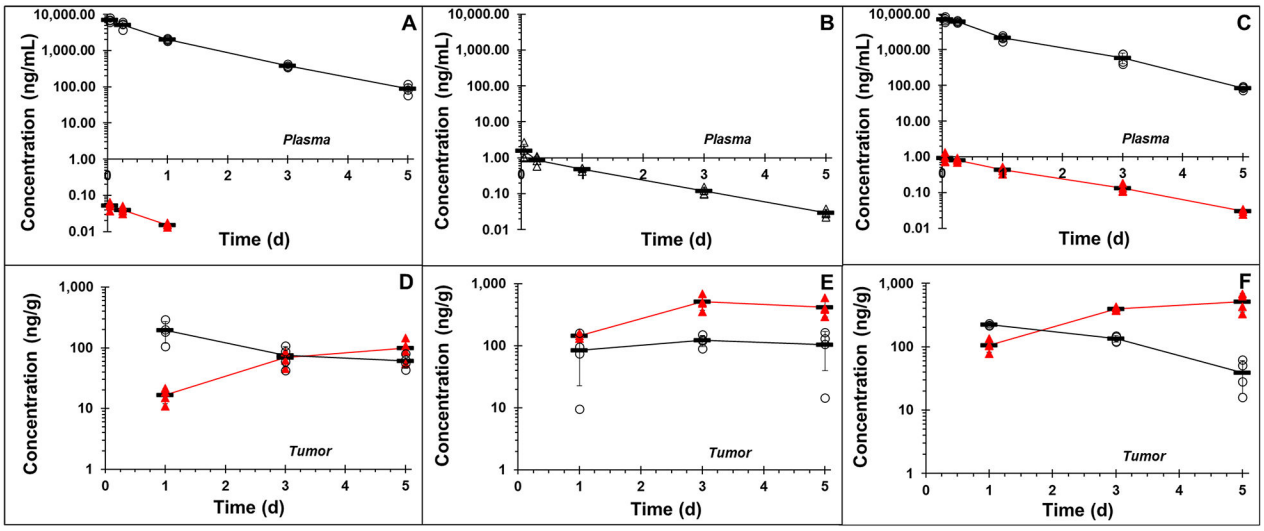

Figure 3:

Concentrations of parent drug (O) and MMAE payload (▲) in ***plasma*** (A,B,C) and ***tumor*** (D,E,F) after IV dosing of 0.8 mg/kg CTT1700 (left column), SMDC **1** (middle column), or SMDC **2** (right column) to NCr nude mice with PC3-PiP tumors.

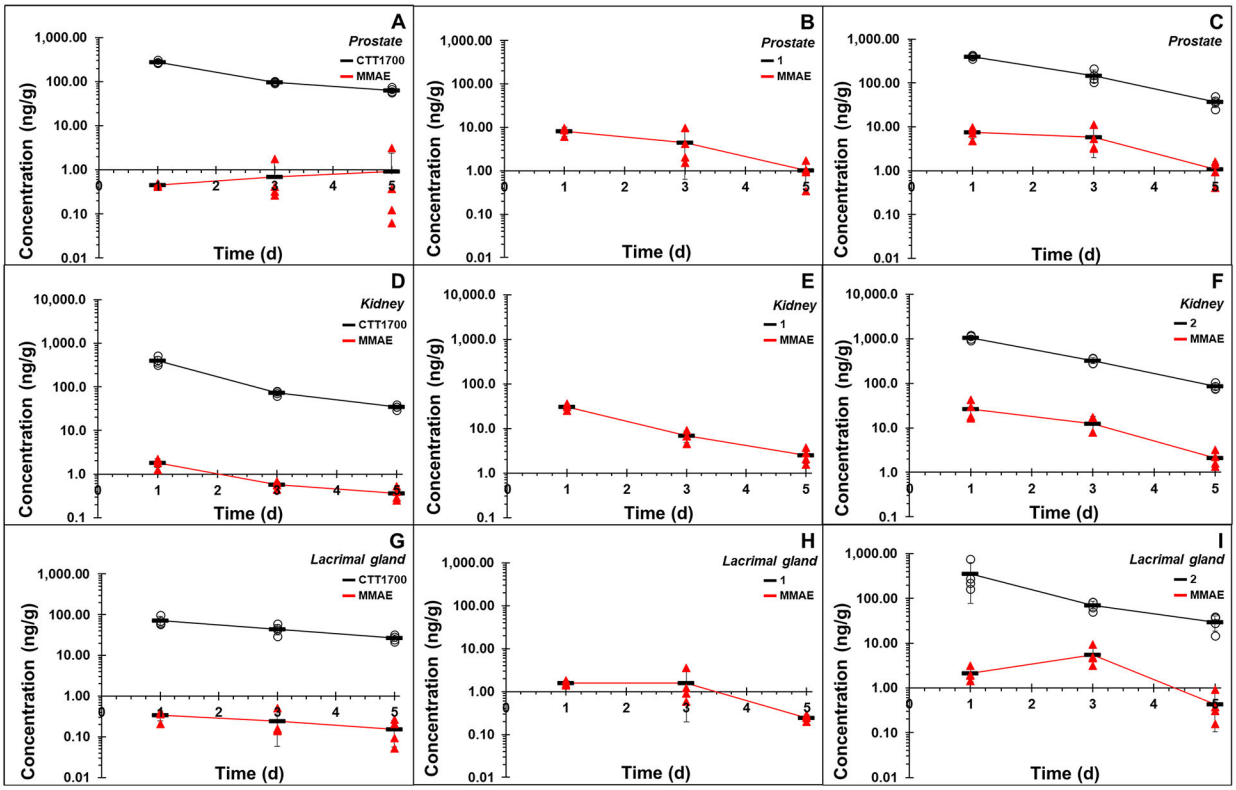

Figure 4:

Concentrations of parent drug (O) and MMAE payload (▲) in ***prostate*** (A,B,C), ***kidney*** (D,E,F) and ***lacrimal gland*** (G,H,I) after IV dosing of 0.8s mg/kg CTT1700 (left column), SMDC **1** (middle column), or SMDC **2** (right column) to NCr nude mice with PC3-PiP tumors.

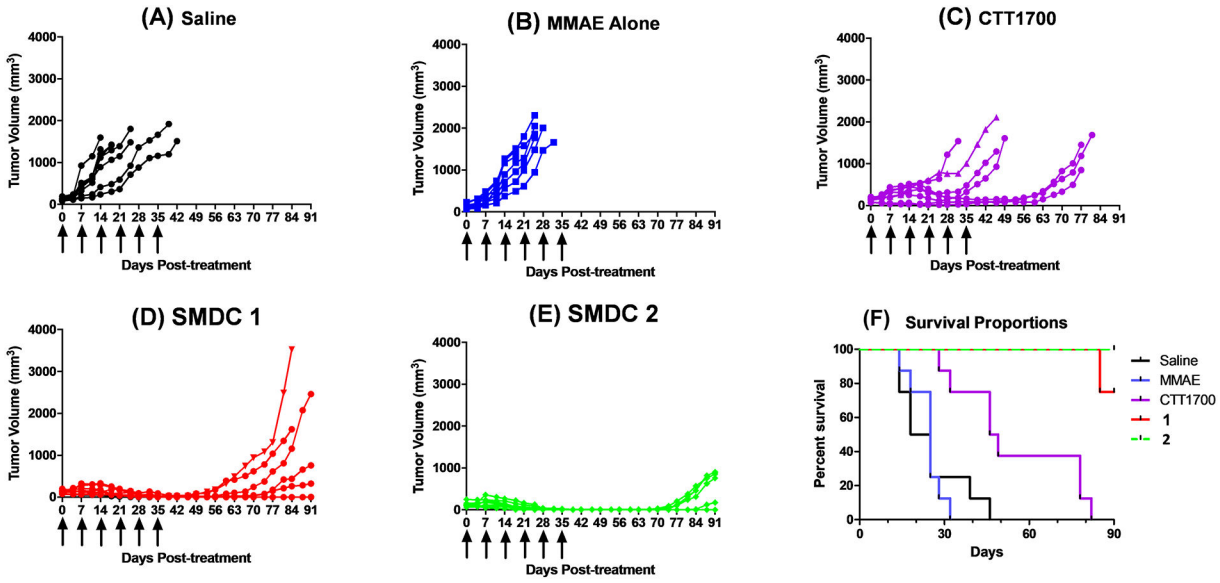

Figure 5:

Therapeutic efficacy of SMDCs **1** and **2** compared to controls **CTT1700**, MMAE alone, and saline. Tumor growth of mice treated with 6 weekly doses of (A) Saline (B) 0.2 mg/kg MMAE (278 nmol/kg) (C) 0.8 mg/kg CTT1700 (SMDC control equipped with slowly cleavable phosphoramidate; 265 nmol/kg) (D) **1** (0.8 mg/kg; 253 nmol/kg) (E) **2** (0.8 mg/kg; 244 nmol/kg) (F) Survival data for mice treated with 6 doses (weekly) of controls, **1**, and **2**.